LIMNOLOGY
and
OCEANOGRAPHY

ASLO

*Limnol. Oceanogr.* 63, 2018, 1605–1621

doi: 10.1002/lno.10795

# Regional and intra-annual stability of dissolved organic matter composition and biolability in high-latitude Alaskan rivers

**Audrey E. Mutschlecner** ,[1]* **Jennifer J. Guerard,**[2] **Jeremy B. Jones,**[1] **Tamara K. Harms**[1]
[1]Department of Biology and Wildlife, Institute of Arctic Biology, University of Alaska Fairbanks, Fairbanks, Alaska
[2]Department of Chemistry and Biochemistry, University of Alaska Fairbanks, Fairbanks, Alaska

## *Abstract*

Nutrient availability and molecular composition of dissolved organic matter (DOM) determine whether the carbon (C) associated with DOM is respired during decomposition or exported from stream networks. High-latitude ecosystems are changing rapidly due to permafrost thaw, shifts in vegetation, and increasing runoff, which alter sources of DOM and nutrients to rivers. To address how changes in the composition of riverine DOM and nutrients may influence C cycling, we quantified biolability of DOM across a latitudinal gradient in Alaska and assessed temporal patterns associated with intra-annual variation in hydrology. We measured biolability under ambient and fertilized conditions and characterized optical and chemical properties of DOM to determine the relative influence of nutrients and molecular composition of DOM on its fate in rivers. Biolability was low, comprising 4% of the DOM pool on average and 0–42% across all sites and seasons. Optical indicators of the molecular composition of the DOM pool were more constant in space and time than bulk concentrations of dissolved C and nutrients, and described a DOM pool dominated by humic-like functional groups. Phosphorus limited biolability at freshet, but biolability was not linked to DOM composition. Strong hydrologic connection of high-latitude rivers to a large pool of soil organic matter likely results in export of recalcitrant DOM to receiving rivers and coasts in this region, contributing to stability of the high-latitude C cycle. However, increased inputs of phosphorus or DOM of greater biolability will likely cause increased respiration of riverine DOM and flux of $CO_2$ to the atmosphere.

Arctic and boreal regions store vast quantities of carbon (C), accounting for nearly 50% of the global pool of soil organic carbon (Hugelius et al. 2014; Köchy et al. 2015; Strauss et al. 2017). Riverine transport and processing of dissolved organic C (DOC) from these ecosystems represent key fluxes between terrestrial, oceanic, and atmospheric C pools (Striegl et al. 2005; Raymond et al. 2007). The composition of dissolved organic matter (DOM) influences its biolability, which determines whether it is susceptible to decomposition by heterotrophic microorganisms that respire DOM and release $CO_2$ to the atmosphere, or whether DOM is recalcitrant to decomposition and subject to hydrologic export (Balcarczyk et al. 2009; Fellman et al. 2009a). Projected changes to C and nutrient cycles in high-latitude ecosystems will affect the sources, quantities, and composition of DOM that reaches rivers (Jones et al. 2005; O'Donnell et al. 2012; Abbott et al. 2014; Drake et al. 2015), influencing the biolability of DOM and its fate within the global C cycle.

Nutrient availability and molecular composition of DOM may both influence rate of decomposition in rivers, but the relative influence of these factors remains unresolved. In this study, we define molecular composition as the relative abundance of functional groups, such as humic-like or protein-like groups, which determine the reactivity of organic molecules. Larger molecules and those with a more aromatic structure require microbial decomposers to allocate more energy to synthesis of extracellular enzymes to break bonds, and polyphenolic molecules can also inhibit enzymatic activity, slowing the rate of decomposition (Sinsabaugh et al. 2013; Mann et al. 2014). In contrast, protein-like functional groups are correlated with high biolability in some rivers (Balcarczyk et al. 2009; Fellman et al. 2009a). However, links between readily measured attributes of the DOM pool and its biolability remain ambiguous. For example, humic functional groups tend to resist decomposition (Qualls and Haines 1992; Fellman et al. 2009b), but can also be somewhat labile (Cory and Kaplan 2012; Kellerman et al. 2015). Observations of DOM composition from a limited number of

*Correspondence: amutschlecner@alaska.edu

Additional Supporting Information may be found in the online version of this article.

high-latitude sites have generated contrasting patterns, including release of aliphatic (nonaromatic) DOM that may be bioavailable where permafrost is thawing (Abbott et al. 2014; Drake et al. 2015; Mann et al. 2015; Spencer et al. 2015), high aromaticity and humic content of DOM in rivers draining ice-rich (O'Donnell et al. 2016) or intact permafrost (Fouché et al. 2017), and strong regional contrasts in the bioavailability in DOM (Larouche et al. 2015). Resolving relationships among DOM composition and biolability would improve estimates of $CO_2$ emission from high-latitude rivers that drain thawing permafrost.

Nutrient content of DOC or availability of inorganic nutrients can influence biolability because microbial decomposers require nutrients such as nitrogen (N) and phosphorus (P) for cellular function. Under nutrient limitation, microbes shift resource allocation from acquisition of C to nutrients, slowing rate of decomposition or yielding higher rates of respiration due to decreased C use efficiency (Hessen and Anderson 2008; Sinsabaugh et al. 2013; Godwin et al. 2017). Limited, but growing evidence suggests that nutrient inputs to high-latitude rivers are increasing. For example, nitrate flux increased nearly fivefold over a decade of observation in an arctic river in Alaska (McClelland et al. 2007), and longer-term observations indicate increasing concentration of inorganic P in the Yukon River (Toohey et al. 2016). Correlation of biolability of DOM with N and P availability in high-latitude rivers indicates potential for increased respiration of DOM under increased nutrient availability (Wickland et al. 2012; Mann et al. 2014). However, previous studies have not experimentally identified nutrient limitation of DOM decomposition across arctic and boreal freshwaters.

High-latitude catchments exhibit strong seasonality in the hydrologic regime, including variation in discharge and depth of groundwater flow, which influences the quantity and composition of DOM reaching rivers (Finlay et al. 2006; O'Donnell et al. 2010, 2012; Mann et al. 2012; Wickland et al. 2012). Limited observations suggest that DOM exported from large Arctic rivers is labile during spring freshet (Holmes et al. 2008; Wickland et al. 2012) when runoff flows through organic-rich, upper soil layers, and yields terrestrially derived, aromatic DOM (Striegl et al. 2007; Spencer et al. 2008; Mann et al. 2012). Wintertime biogeochemistry of high-latitude rivers is sparsely described, but high biolability of DOC has been measured during winter in the Yukon River and its large tributaries (Wickland et al. 2012). Corresponding observations of composition indicate that the DOM pool of these rivers contains a high proportion of hydrophilic compounds and a low DOC : dissolved organic nitrogen (DON) ratio in winter (Striegl et al. 2007; O'Donnell et al. 2012), characteristics positively correlated with biolability in some studies (Wickland et al. 2007, 2012; Kiikkilä et al. 2013). Most estimates of biolability in high-latitude rivers have been made during summer, but many of the climate-induced changes to DOM availability and processing might occur outside of the growing season, including more rapid soil thaw, earlier snowmelt, and reduced ice cover (Stone et al. 2002; Brabets and Walvoord 2009; Euskirchen et al. 2010; Stackpoole et al. 2017).

The objectives of this study were to describe temporal patterns in DOM composition and biolability across a boreal-arctic gradient, and to determine the relative influences of nutrient availability and molecular composition of DOM on biolability. To address these objectives, we measured the molecular composition and biolability of DOM from rivers draining spatially discontinuous to continuous permafrost in Alaska. Rivers were sampled routinely for a year, including winter, for which there are few available estimates of DOM biolability. DOM composition was characterized by optical properties (absorbance and fluorescence) and chemical analysis (organic C, N, and P concentrations). We incubated water to estimate biolability, measured as the fraction of DOC that is susceptible to microbial decomposition, and the response of biolability to factorial fertilizations with N and P. We hypothesized that nutrient availability constrains the decomposition rate when microbial decomposers are nutrient-limited. Alternatively, the molecular composition of DOM might constrain biolability due to the energy demands of decomposing large and complex molecules.

## Methods

### Site description and sampling

We sampled rivers spanning an arctic-boreal gradient in interior Alaska eight times between April 2015 and May 2016. Contributing areas of the rivers ranged 61–3316 $km^2$, and all are $5^{th}$–$7^{th}$ order. Permafrost underlying the watersheds ranges from spatially discontinuous in the south to continuous in the north (Fig. 1, Ferrians 1998). South of the Brooks Range, vegetation is typical of the boreal forest (cover dominated by black spruce [*Picea mariana*], white spruce [*Picea glauca*], paper birch [*Betula neoalaskana*], and quaking aspen [*Populus tremuloides*]), although tundra occurs at high elevations or low topographic relief. Tundra occurs north of the Brooks Range, dominated by tussock-forming sedges [*Eriophorum* spp.], mosses, and dwarf shrubs [*Betula nana* and *Salix pulchra*]. Harms et al. (2016) describes physical and vegetative attributes of the study catchments in further detail. Average annual air temperature ranges from −6°C for the southern sampling locations to −10°C for the northern-most sampling location and average annual precipitation ranges from 460 mm for the southern sites to 320 mm for the northern sites (Bonanza Creek LTER Climate Database 2016; Toolik Environmental Data Center Team 2016).

Rivers in this region exhibit strong seasonal patterns in discharge with low flow or bedfast ice during winter and maximum annual discharge during spring snowmelt (Brabets et al. 2000). Sampling dates included April (pre-snowmelt),

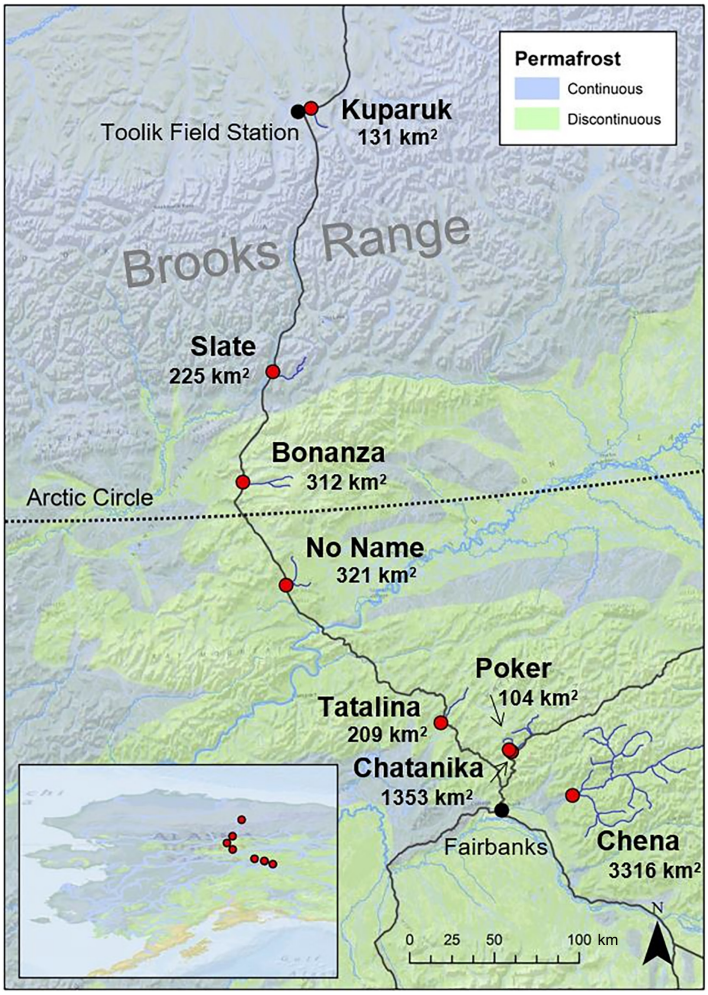


**Fig. 1.** Locations of sampled rivers in northern Alaska. Red points indicate sampling locations with catchment areas indicated. The stream network upstream of each sampling point is shown in dark blue and major roads are indicated by black lines. Permafrost data are from Ferrians (1998). [Color figure can be viewed at wileyonlinelibrary.com]

May (snowmelt), June (growing season), August/early September (fall), and November 2015 (winter) and February (winter), April, and late April/early May 2016 (snowmelt; Supporting Information Table 1). An ice auger was used to collect under-ice samples in winter, and overflow (water discharged above bedfast ice that is present throughout the valley bottom) was collected when present. Samples were collected in acid-washed 1-L bottles, transported on ice, filtered to 0.7 $\mu$m (Whatman GF/F) within 24 h of collection, and filtered to 0.45 $\mu$m (Pall GN-6) and 0.2 $\mu$m (Whatman Nuclepore Polycarbonate Membrane Filter) within 48 h of collection. Analysis of dissolved solute concentrations (*see* "Chemical analysis" section) were performed on 0.7 $\mu$m-filtered samples; optical properties were determined on 0.45 $\mu$m-filtered subsamples, as is standard for this analysis (Cory and McKnight 2005); and incubation to determine biolability of DOM was performed on 0.2 $\mu$m-filtered samples, which removes the majority of microbial cells and therefore all particulate C.

### Chemical analysis

Each sample was analyzed for concentration of DOC, total dissolved N (TDN), ammonium ($NH_4^+$), total dissolved phosphorus (TDP), and major anions and cations. DOC concentration was measured as nonpurgeable organic C by nondispersive infrared gas analysis on a total organic C analyzer (TOC-L CPH, Shimadzu Scientific Instruments, limit of quantification [LOQ] = 8 $\mu$M) connected to a nitrogen monoxide chemiluminescence analyzer (TNM-L, LOQ = 1.4 $\mu$M). $NH_4^+$ was measured by automated colorimetry (Smartchem 170, Westco Scientific Instruments, LOQ = 0.6 $\mu$M) using the phenol hypochlorite method (Solórzano 1969). Anion and cation concentrations were measured on an ion chromatograph (Dionex ICS 2100) equipped with AS18 columns for anions (LOQ = 0.01 $\mu$M $NO_3^-$, 0.25 $\mu$M $Cl^-$, 0.01 $\mu$M $SO_4^{2-}$) and CS16 columns for cations (LOQ = 0.5 $\mu$M $Na^+$, 0.3 $\mu$M $K^+$, 1.2 $\mu$M $Mg^{2+}$, 1.5 $\mu$M $Ca^{2+}$). TDP was measured following persulfate digestion using the molybdate blue method

(Murphy and Riley 1962) on a spectrophotometer with a 5-cm cell (Shimadzu UVmini 1240, Shimadzu Scientific Instruments, LOQ = 0.02 $\mu$M). Soluble reactive phosphorus was measured for a subset of the samples and was at or near the detection limit, indicating that at most sites and times, TDP is largely organic. Nitrite is not detectable in the study rivers. Therefore, concentration of DON was determined as: DON = TDN − [$NO_3^-$-N + $NH_4^+$-N]. A proxy for groundwater inputs (GW) was calculated as the molar sum of $Na^+$, $Mg^{2+}$, $Cl^-$, and $SO_4^{2-}$, all of which are present in high concentration in local groundwater and behave conservatively in this region (O'Donnell et al. 2010; Toohey et al. 2016). When measured values were below the LOQ, the average of the LOQ and zero was used in data analysis.

**DOM absorbance and fluorescence**

To characterize DOM composition, we measured absorbance of UV and visible light as well as fluorescence spectra using a fluorometer (Jobin-Yvon Horiba Aqualog-800-C, Horiba Instruments) with a 1-cm quartz cuvette (Firefly Scientific). Excitation-emission matrices (EEMs) were collected over an excitation range of 240–600 nm every 3 nm and an emission range of 247–604 nm every 2.33 nm with an integration time of 0.1 s and a medium gain. Data were instrument-corrected, blank-subtracted, Raman-normalized, and corrected for inter-filter effects. Parallel factor analysis (PARAFAC) was applied to resolve fluorescing components using the DOMFluor toolbox (version 1–7, Stedmon and Bro 2008) in MATLAB (version R2015b, MathWorks). The PARAFAC model was based on the 52 samples presented here, as well as additional samples to increase the power of the model, including a set of 45 samples of leachates derived from plant species common to the boreal region included in this study (Mutschlecner et al. 2017), and 132 stream water samples that had been incubated and/or acidified, for a total of $n = 229$ samples supporting the model. A model including five components was best supported by the data as determined by inspection of residuals for random variation and model validation (Supporting Information Fig. 1). Model validation was conducted following the approach of Stedmon et al. (2003), and included split-half analysis, which compares PARAFAC models made on two halves of the data, and random initialization, which performs 10 iterations with different starting estimates to confirm that the least squares result was not a local minimum (Supporting Information Fig. 2). To identify the chemical attributes of the components identified by PARAFAC analysis, excitation and emission spectra were compared with published data using the OpenFluor database. PARAFAC components 1–4 were matched to previously described components in the OpenFluor database using a 0.95 Tucker convergence coefficient (Murphy et al. 2014). Component 5 visually appeared to consist of two components, but the model was unable to resolve them separately (Supporting Information Fig. 1) and component 5 did not match components published in OpenFluor, even when the two portions of the component were compared separately, but was instead visually matched to previously reported excitation and emission curves (Cory and McKnight 2005).

In addition to the PARAFAC analysis of EEMs, several indices were calculated from both EEMs and absorbance of light in the UV-visible range. Fluorescence index (FI) describes the contribution of terrestrial and microbial sources to the DOM pool and is calculated as the ratio of emission intensities at 470 nm and 520 nm at exitation 370 nm, with values of 1.4 indicating terrestrially derived fulvic acids and 1.9 indicating microbially derived fulvic acids (McKnight et al. 2001; Cory et al. 2010). Humification index (HIX) is calculated as the area under the emission spectra 435–480 nm divided by the sum of the areas under the 300–345 nm and 435–480 nm regions at excitation at 254 nm, and ranges from 0 to 1, with higher values indicating greater humic content (Ohno 2002). Biological index (BIX) indicates autotrophic productivity and is calculated as the ratio of emission intensities at 380 nm and 430 nm at exitation 310 nm, with values > 1 indicating recently produced DOM of autochthonous origin (Huguet et al. 2009). Freshness index ($\beta : \alpha$) indicates the relative contribution of recently produced DOM and is calculated as the ratio of emission intensity at 380 nm divided by the maximum emission intensity between 420 nm and 435 nm at excitation 310 nm, with higher values indicating a greater proportion of recently produced DOM (Parlanti et al. 2000; Wilson and Xenopoulos 2009). From absorbance of light in the UV-visible range, we calculated specific ultraviolet absorbance (SUVA) at 254 nm, which is associated with greater aromatic content, by dividing the absorbance at 254 nm by DOC concentration (Weishaar et al. 2003), and spectral slope ratio (SR), which is negatively correlated with DOM molecular weight and aromaticity, as the ratio of the slope from 275 nm to 295 nm to the slope from 350 nm to 400 nm with log-linear fits (Helms et al. 2008).

**DOC biolability**

Biolability of DOC, defined as the fraction of DOC that is available to microbial decomposers, was quantified in laboratory-based incubations of river water inoculated with a common microbial consortium. Water from each river was filtered to 0.2 $\mu$m to remove the majority of microorganisms and 120 mL was added to a glass jar that had been ashed to remove organic C. An approximately equal volume of headspace prevented anoxia during incubation. Microbial inocula included both water column and sediment-derived microbial communities. On each sampling date, a slurry of sediment and water was collected from the Chena River. In November and February, when ice cover prevented collection of sediment, we used sediment collected in October 2015 and frozen until use. The sediment slurry was shaken, filtered to 0.7

$\mu$m, and then to 0.2 $\mu$m until each filter clogged. The 0.2-$\mu$m filters were placed in a beaker of deionized water (18 MΩ) at a ratio of 1 filter to 10 mL water. We also added an equivalent number of clogged 0.2 $\mu$m filters following filtration of the river water collected on each sampling date to include microbes present in the water column. The resulting inoculum was added to each water sample at a ratio of 1 mL inoculum:100 mL sample water. Preliminary tests indicated that reproducibility of measured DOC biolability was greater using inocula prepared at this ratio compared to more dilute inocula. Additionally, incubation of 10 mg $L^{-1}$ glucose in unfertilized river water resulted in loss of 55% ± 10% DOC, on average, within 21 d, indicating that the inoculum was viable.

Biolability assays included unfertilized controls, as well as fertilization with inorganic N, P, and both nutrients to determine whether nutrients limited decomposition. Nutrient concentrations were selected to relieve possible nutrient limitation of decomposition and to match the Redfield ratio of 16 : 1 for N : P. The concentration of N in the N treatment was 1 mM greater than ambient (50 : 50 N as $NH_4Cl$ and $KNO_3$). The concentration of P in the P treatment was 0.0625 mM greater than ambient (added as $KH_2PO_4$). An equivalent volume of deionized water was added to unfertilized controls. Three replicates of each nutrient treatment were incubated.

Biolability was estimated as loss of DOC over 21 d. Samples were incubated in the dark, at laboratory temperature (25°C), enabling comparison among sites and sampling dates, and with estimates of DOC biolability from the literature. All samples were filtered to 0.2 $\mu$m upon collection from the incubations and were immediately acidified and refrigerated until analysis. Samples were analyzed for DOC concentration as previously described. Absolute loss of DOC was calculated as the change in DOC concentration between day 0 and day 21, and percent loss was calculated by dividing absolute loss by the initial DOC concentration.

**Statistical analysis**

We applied statistical analyses to quantify spatial and temporal variation in DOM composition and biolability of DOC, and potential drivers of these patterns. First, we used the coefficient of variation (CV) summarized across catchments (spatial CV) and across sampling dates within each catchment (temporal CV) to compare the magnitude of variation in each measured attribute of river water. We contrasted water chemistry among sampling dates for each river using mixed effects models (*lme4* package; Bates et al. 2015) that included site as a random effect to account for variance among sites. Sampling date was included as a fixed effect in these models with Tukey's honestly significant difference tests applied post hoc to test for differences among sampling dates ($\alpha = 0.05$).

We statistically evaluated the effects of nutrient availability on biolability of DOC. To determine whether nutrients limit decomposition of DOC, we examined temporal variation in the effects of experimental fertilization (control, N, P, and N + P) on DOC loss using linear mixed effects models. Separate means (based on laboratory replicates) for each site and date were incorporated as a random effect. We contrasted models that included fixed effects of sampling date, nutrient treatment, and their interaction using Akaike's information criterion corrected for small sample size (AICc) to select a final model that was most parsimonious and best supported by the data. Residuals were visually inspected for normality and constant variance. We estimated marginal $R^2$, the variance explained by fixed effects and conditional $R^2$, variance explained by random and fixed effects, as metrics of model fit using the *MuMIn* package (Barton 2016).

We constructed multiple regression models to explore the chemical attributes correlated with biolability in the unfertilized assays. Candidate predictor variables included DOC and nutrient concentrations (total nitrogen [TN], DON, $NO_3^-$, $NH_4^+$, TDP), a proxy for groundwater inputs based on conservative solutes (GW), optical indices of DOM composition (SUVA, SR, FI, HIX, BIX, $\beta : \alpha$), and the five components from the PARAFAC model of EEMs. Predictor variables were centered and standardized by subtracting the mean and dividing by standard deviation prior to analysis. Predictors with correlation coefficients $> |0.5|$ were not allowed in the same model. Models included site as a random effect. Initial models indicated that ambient DOC concentration was the dominant correlate of both absolute DOC loss and total percent DOC loss. To further explore the effects of other potential predictors of DOC biolability, we attempted to model the residuals of the relationship between biolability and DOC concentration using the multiple regression approach described above.

Following a similar approach, we applied multiple logistic regression analysis to explore the chemical attributes correlated with an enhancement of biolability by nutrient fertilization. The binary response represented whether DOC loss was greater in the amended assay compared to unamended control (hereafter "N response" and "P response"). Predictor variables were the same as the potential correlates of biolability described previously and we considered multivariate models comprised of up to three predictors. In these logistic models, the random effect of site did not explain any variance and was therefore dropped from models.

Finally, we used multiple regression to address factors that may influence spatial heterogeneity of biolability among the rivers. Attributes of catchments including slope, active layer depth, and vegetation (indicated by % cover of black spruce) were included as potential predictors of biolability on sampling dates showing maximum biolability (April and May). Catchment attributes were described by Harms et al. (2016), with the exception of active layer depth

from the Kuparuk basin, which was reported by the CALM network (https://www2.gwu.edu/~calm/data/north.html). We considered models with a maximum of two predictors and included date as a random effect. The Kuparuk River demonstrated strong leverage in models that included active layer depth, with thaw 2–3 times shallower than other sites, and we were therefore unable to fit a reliable relationship between active layer depth and biolability. All statistical analyses with the exception of PARAFAC analysis (described above) were conducted in R (version 3.3.1, R Core Team 2016).

## Results

### Spatial and temporal patterns in stream chemistry

DOC concentration was greatest for the sampling events in May, which occurred during spring freshet, and lowest during February, when samples were collected from beneath ice or as overflow (Fig. 2a). A second peak in DOC concentration occurred for most sites in August, coinciding with precipitation and increased discharge (Supporting Information Fig. 3). DON concentration generally followed patterns in DOC (Fig. 2f). Average TDP concentration was approximately four times greater during spring freshet in May than during summer baseflow in June or winter baseflow in November and February (Fig. 2e). The proxy for groundwater inputs (GW) tended to increase throughout the winter and declined during freshet, decreasing nearly 60% between April and May 2016, although statistical contrasts among individual dates were largely nonsignificant (Fig. 2b). A nutrient-rich sample was collected from overflow on the still ice-covered Kuparuk River in April 2016 and was withheld from statistical analysis due to concentrations of labile DOC and nutrients that were nearly 10 standard deviations greater than mean values.

Large, humic molecules indicative of soil organic matter dominated the DOM pool in nearly all samples, and the relative contribution of these molecules tended to be greatest during snowmelt. FI values ranged between 1.4 and 1.6 (Table 1) for all but one sample, indicating terrestrial plants as the ultimate source of most DOM (McKnight et al. 2001). Across all sites and sampling events, low BIX values ($< 1$) indicated little contribution of recent autotrophic production to the DOM pool (Huguet et al. 2009). Significant declines in $\beta : \alpha$ during snowmelt indicated that DOM exported during snowmelt was processed, rather than freshly produced (Fig. 2i). Several additional metrics showed complementary, though nonsignificant, trends indicating a flush of humic DOM to rivers during snowmelt, followed by a gradual decline in the relative contribution of this material from summer through winter, with corresponding increase in the relative contributions of microbial or autochthonous production. These include FI, which indicated declining humic content and increasing relative abundance of microbially derived DOM after snowmelt; HIX, which indicated a similar decline in humic molecules, and $\beta : \alpha$, which showed increased input of more recently produced DOM following snowmelt (Fig. 2g–i).

Five fluorescing components of DOM were identified from PARAFAC analysis of EEMs. Comparisons with the OpenFluor database indicate that Component 1 (Kothawala et al. 2014) and Component 2 (Shutova et al. 2014) are humic-like (Table 2); Component 3 is a high molecular weight fraction of terrestrially derived DOM (Kothawala et al. 2014); and Component 4 is protein-like (Dainard et al. 2015). Component 5 was visually matched to the fluorescence spectra of an uncharacterized component previously observed by Cory and McKnight (2005) in samples from a range of aquatic environments including Arctic lakes. Humic-like components (C1, C2, and C3) represented 88% of fluorescent component loadings, on average (Fig. 3). The loading of Component 4 (protein-like) tended to be largest during April of both years of the study (Fig. 3), indicating a higher proportion of protein-like DOM at or just before the onset of snowmelt. Despite these temporal patterns, intra-annual variation was lower for metrics of DOM composition than for bulk concentrations of solutes, shown by the CV summarized across sampling events (Table 1).

Spatial variation was greater than temporal variation for bulk solute concentrations (DOC, DON, TDP, and $NO_3^-$), whereas temporal variation exceeded spatial variation for molecular composition of DOM, as assessed by CVs (Table 1). DOC concentration varied fourfold across sites spanning the arctic-boreal gradient. HIX tended to be lower for the arctic sites (Bonanza, Slate, and Kuparuk), and $NO_3^-$ concentration was approximately three times higher for the southernmost sites (Chena, Chatanika, and Poker) than the other sites (Table 1, Supporting Information Fig. 4).

### Spatial and temporal patterns in DOM biolability

Biologically labile DOC represented a small fraction of the total DOC pool in nearly all samples measured. Total loss of DOC in unfertilized incubations ranged from 0% to 42% of the DOC pool, with an average of 4% (Fig. 4). Although biolability was nearly five times greater in April and May than for the rest of the year, variation among sites contributed to lack of a statistical difference in biolability among dates, indicated by Tukey's post-hoc comparisons. The primary chemical correlate of biolability was ambient DOC concentration, which explained greater than 65% variation in biolability in terms of fractional loss of DOC (Fig. 5). DOC concentration similarly explained absolute loss of DOC (Absolute loss $[\mu M] = 0.07 * \text{DOC} - 27$, marginal $R^2 = 0.68$ and conditional $R^2 = 0.79$), with site as a random effect. Using ambient nutrient chemistry and DOM composition as potential predictors, multiple regression models on the residuals of the relationship of DOC concentration and biolability

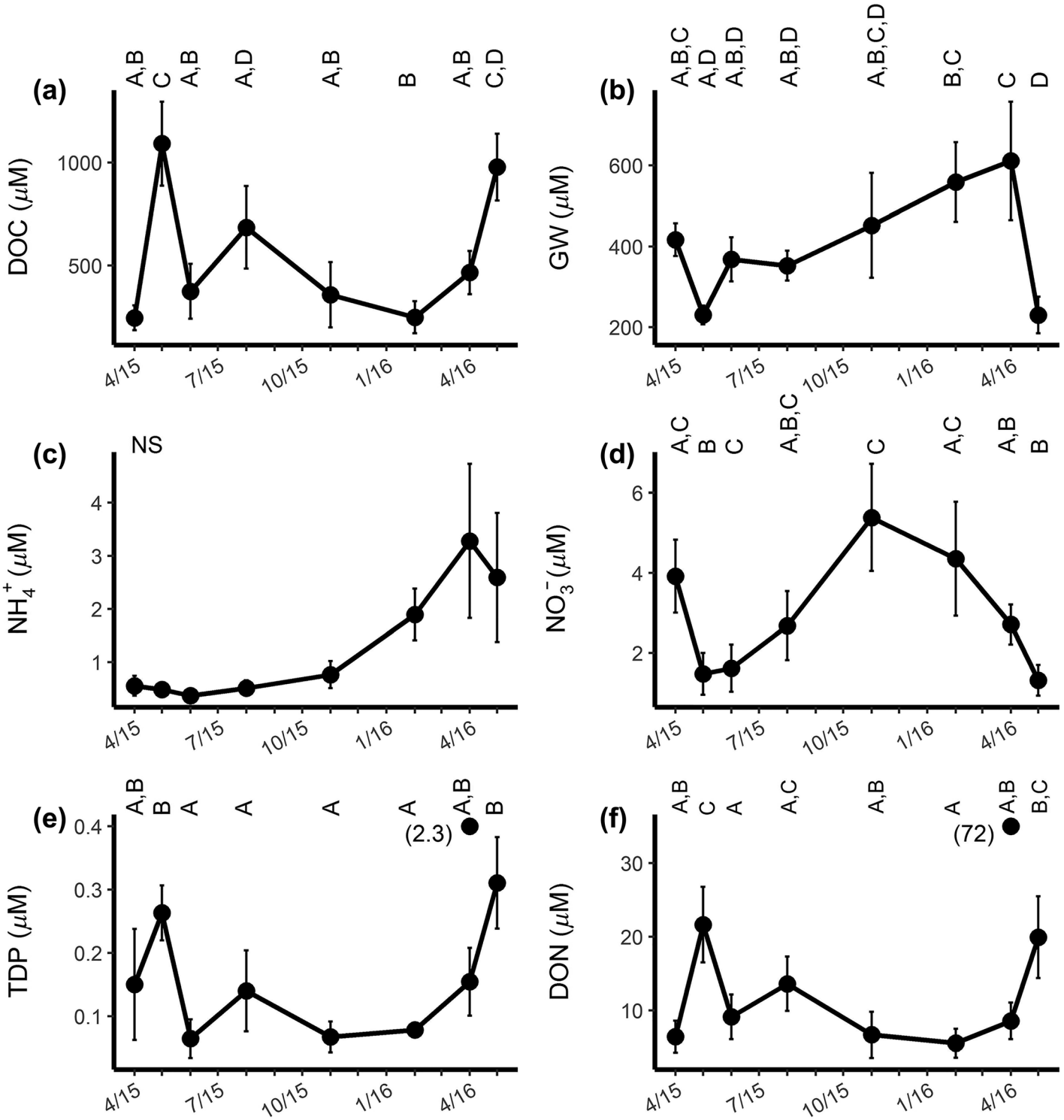


**Fig. 2.** Temporal patterns in DOM composition and bulk chemistry of rivers. Plots display concentrations of DOC, a proxy for groundwater contribution based on the sum of conservative ions (GW), ammonium ($NH_4^+$), nitrate ($NO_3^-$), TDP, and DON. Metrics of DOM composition shown are FI, HIX, BIX, SUVA, and spectral SR. Biolability represents total percent loss of DOC from incubations. Points are means across all sampled rivers with error bars indicating one standard error (*see* Supporting Information Table 1 for rivers sampled on each date). Points with arrows indicate values for an outlier sampled as overflow from the Kuparuk River. Letters indicate significant differences between sampling events based on Tukey's honestly significance difference, following linear mixed effects models that included site as a random effect. NS indicates not significant. (Continued on next page).

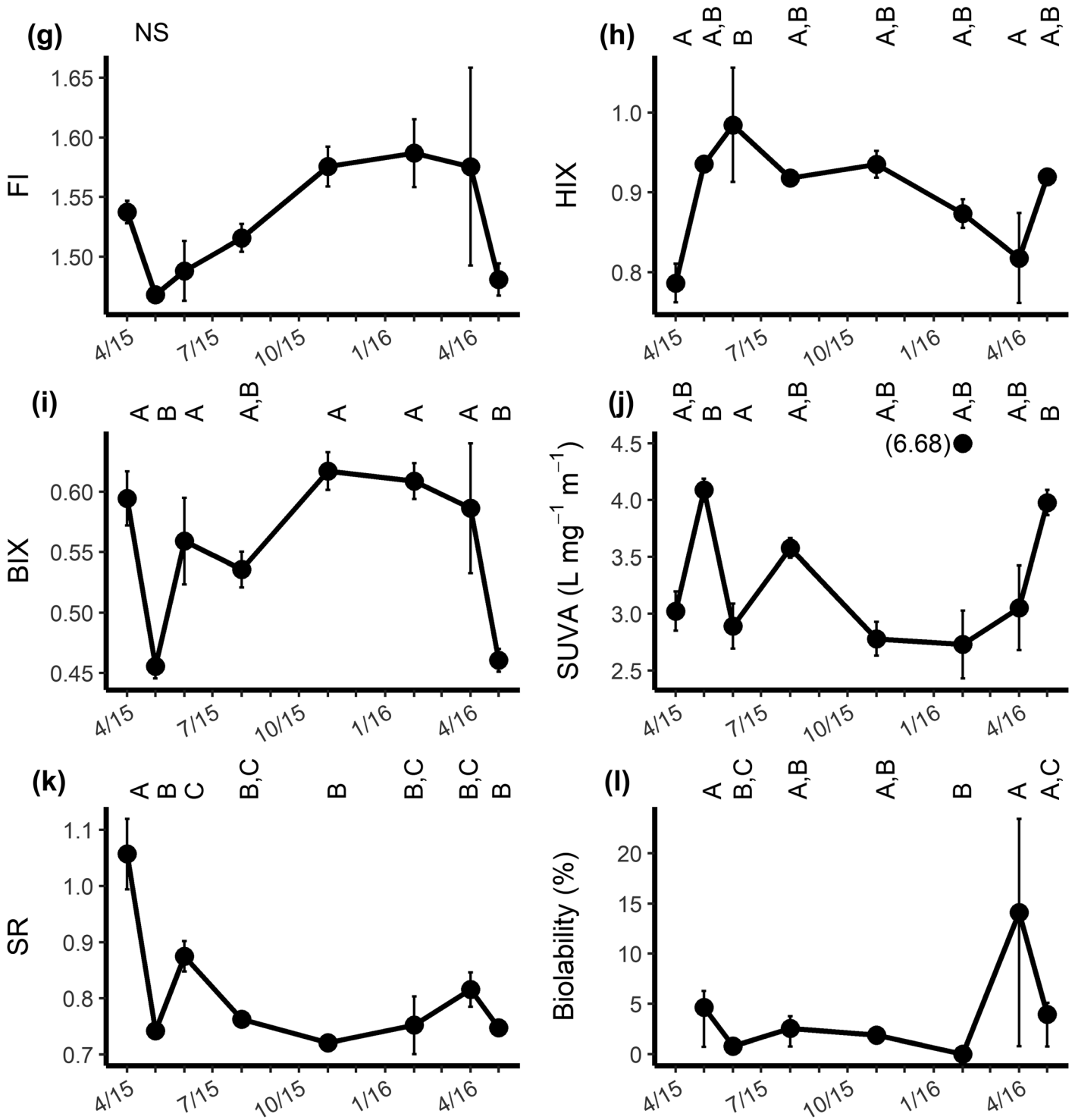


**Fig. 2.**

explained little of the remaining variation in biolability ($R^2 < 0.1$). Finally, variation in biolability among rivers was best explained by a positive relationship with mean catchment slope (Fig. 6), based on the data representing the dates of maximum biolability (April and May).

Nutrient fertilization assays revealed that P limits biolability during snowmelt. The effects of nutrient fertilization and sampling date on biolability were determined by comparison of models containing fixed effects of nutrient treatment, sampling event, and their interaction, with a random mean

**Table 1.** DOC biolability, bulk chemistry, and optical properties of DOM in the eight rivers included in this study, listed from south to north. Values are reported as mean and CV summarized across the sampling events at each site, with number of sampling events indicated for each site. Average temporal CV is summarized across all sites, and the CV of means across the study period indicates spatial variance. CVs are not available for Slate Creek as no DOC loss was observed. Included are the proxy for groundwater inputs (GW), which represents a sum of conservative ions, FI, HIX, BIX, freshness index ($\beta : \alpha$), SUVA, and spectral SR. Stoichiometric ratios are given in molar units.

| | Latitude | Longitude | Catchment slope (°) | DOC loss (%) | DOC loss ($\mu$M) | DOC ($\mu$M) | DON ($\mu$M) | $NH_4^+$ ($\mu$M) | $NO_3^-$ ($\mu$M) | TDP ($\mu$M) |
|---|---|---|---|---|---|---|---|---|---|---|
| Chena ($n = 8$) | 64.877 | −146.755 | 14.4 | 2.2 (119) | 11 (77) | 388 (67) | 6.4 (83) | 1.8 (204) | 4.2 (40) | 0.1 (67) |
| Chatanika ($n = 8$) | 65.141 | −147.457 | 11.9 | 4.7 (76) | 36 (87) | 419 (71) | 8.2 (70) | 0.9 (110) | 4.0 (50) | 0.1 (83) |
| Poker ($n = 8$) | 65.152 | −147.485 | 11.5 | 0.9 (85) | 5 (101) | 454 (79) | 7.5 (75) | 0.8 (74) | 5.6 (31) | 0.1 (87) |
| Tatalina ($n = 7$) | 65.328 | −148.312 | 6.8 | 4.7 (72) | 84 (93) | 1197 (59) | 25.2 (73) | 2.0 (109) | 1.0 (56) | 0.2 (76) |
| No name ($n = 3$) | 66.116 | −150.166 | 4.4 | 1.8 (169) | 28 (161) | 1332 (19) | 31.6 (15) | 1.3 (122) | 0.3 (62) | 0.5 (46) |
| Bonanza ($n = 5$) | 66.676 | −150.660 | 9.6 | 3.5 (40) | 18 (27) | 421 (50) | 9.2 (39) | 0.4 (0) | 1.4 (103) | 0.1 (76) |
| Slate ($n = 6$) | 67.254 | −150.177 | 13.0 | 0.0 | 0.0 | 324 (85) | 7.3 (66) | 0.6 (56) | 1.4 (28) | 0.1 (95) |
| Kuparuk ($n = 7$) | 68.647 | −149.412 | 6.6 | 14.4 (130) | 96 (88) | 621 (72) | 23.4 (97) | 2.3 (133) | 0.7 (96) | 0.6 (141) |
| Average temporal CV (%) | | | | 99 | 90 | 63 | 65 | 101 | 58 | 84 |
| Average spatial CV (%) | | | | 110 | 129 | 70 | 88 | 74 | 74 | 97 |

| | C : N | C : P | GW ($\mu$M) | FI | HIX | BIX | $\beta : \alpha$ | SUVA (L $mg^{-1}$ $m^{-1}$) | SR |
|---|---|---|---|---|---|---|---|---|---|
| Chena | 14 (63) | 4274 (38) | 404 (23) | 1.53 (5) | 0.90 (11) | 0.57 (13) | 0.55 (12) | 3.16 (18) | 0.82 (10) |
| Chatanika | 16 (72) | 6463 (90) | 366 (26) | 1.51 (4) | 0.94 (14) | 0.53 (15) | 0.51 (13) | 3.34 (23) | 0.81 (11) |
| Poker | 14 (82) | 3918 (47) | 278 (40) | 1.48 (2) | 0.94 (15) | 0.51 (15) | 0.49 (14) | 3.38 (18) | 0.78 (12) |
| Tatalina | 36 (25) | 7407 (35) | 660 (55) | 1.53 (3) | 0.95 (4) | 0.54 (11) | 0.53 (11) | 3.60 (12) | 0.75 (5) |
| No name | 39 (3) | 2869 (41) | 429 (45) | 1.52 (2) | 0.94 (1) | 0.56 (8) | 0.55 (8) | 3.96 (7) | 0.78 (4) |
| Bonanza | 27 (49) | 5253 (54) | 216 (42) | 1.46 (4) | 0.87 (10) | 0.51 (19) | 0.49 (17) | 3.72 (19) | 0.82 (17) |
| Slate | 20 (59) | 4909 (86) | 419 (33) | 1.59 (12) | 0.82 (15) | 0.58 (24) | 0.54 (22) | 3.17 (27) | 0.89 (20) |
| Kuparuk | 27 (60) | 2873 (68) | 299 (71) | 1.54 (4) | 0.84 (12) | 0.57 (17) | 0.55 (17) | 3.37 (48) | 0.82 (27) |
| Average temporal CV (%) | 52 | 57 | 42 | 5 | 10 | 16 | 14 | 22 | 13 |
| Average spatial CV (%) | 59 | 50 | 42 | 4 | 7 | 10 | 9 | 18 | 7 |

**Table 2.** Fluorescent components in streamwater DOM as identified by PARAFAC analysis of EEMs.

| Component | Excitation max nm | Emission max nm | Description | Reference |
|---|---|---|---|---|
| C1 | 340 | 460 | Humic-like | C1, Kothawala et al. (2014) |
| C2 | 300 | 390 | Humic-like | C2, Shutova et al. (2014) |
| C3 | 290/400 | 500 | High molecular weight fraction of terrestrially derived humic-like material | C3, Kothawala et al. (2014) |
| C4 | 275 | 320 | Protein-like | C4, Dainard et al. (2015) |
| C5 | 315 | 450 | Characteristics unknown | C10, Cory and McKnight (2005) |

for each site and sampling date combination. AICc values indicated strongest support for a model including nutrient treatment as the only fixed effect (Supporting Information Table 2). However, the explanatory value of the nutrient-only model was low (marginal $R^2 < 0.1$), and therefore, the model including nutrient treatment, sampling date, and their interaction was selected. Overall, P addition increased DOC loss by $3.0\% \pm 0.5\%$ or $25 \pm 8$ $\mu$M over unfertilized

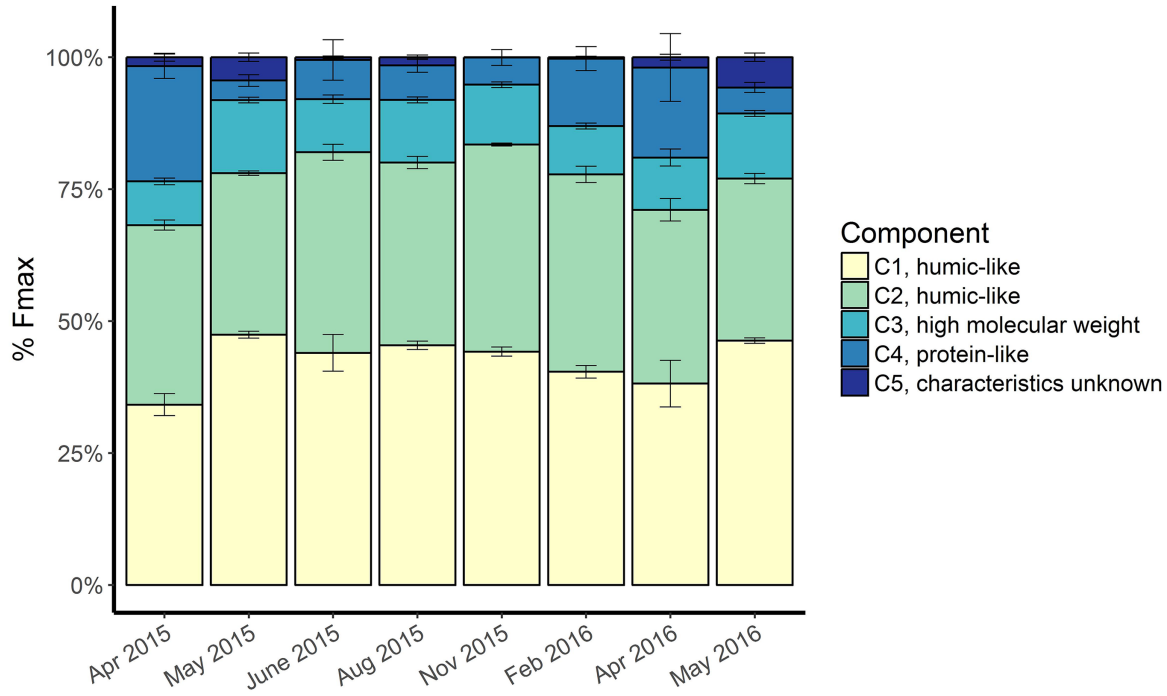


**Fig. 3.** Temporal patterns in DOM composition indicated by components from PARAFAC analysis of EEMs. Fmax represents fluorescence intensity, the fluorescence emission at the wavelength of maximum intensity, and error bars indicate one standard error. [Color figure can be viewed at wileyonlinelibrary.com]

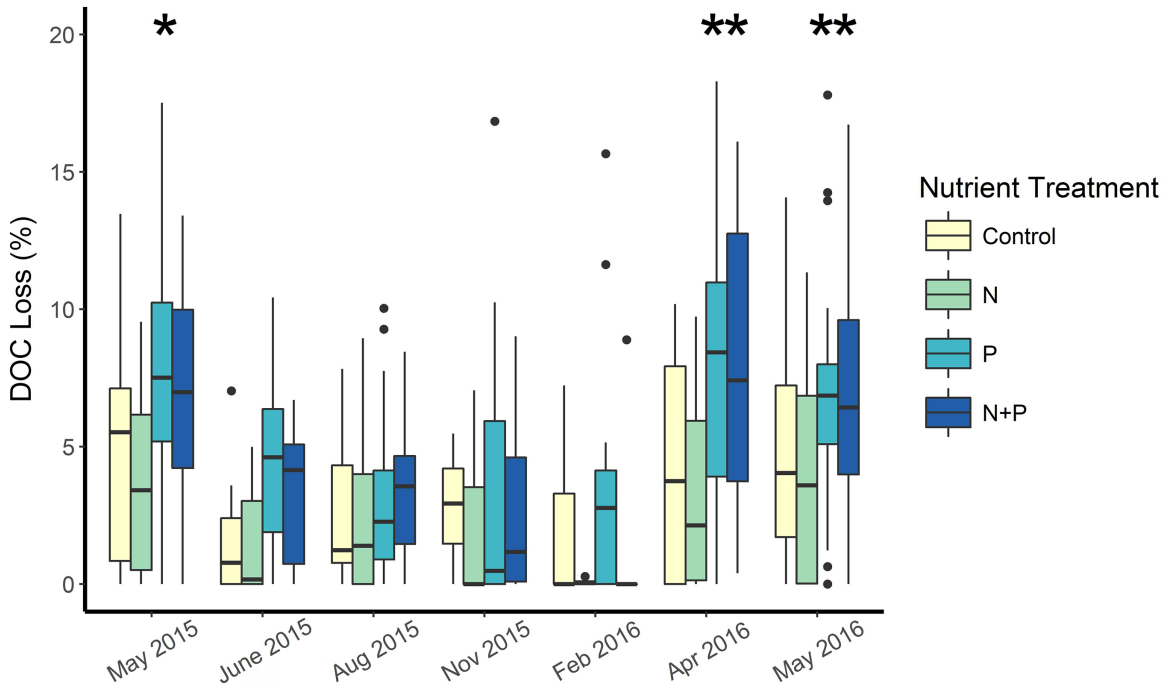


**Fig. 4.** DOC biolability in streamwater incubated under ambient and nutrient-amended conditions. Asterisks indicate a significant effect of nutrient addition, determined by comparisons to the control treatment within each sampling event. [Color figure can be viewed at wileyonlinelibrary.com]

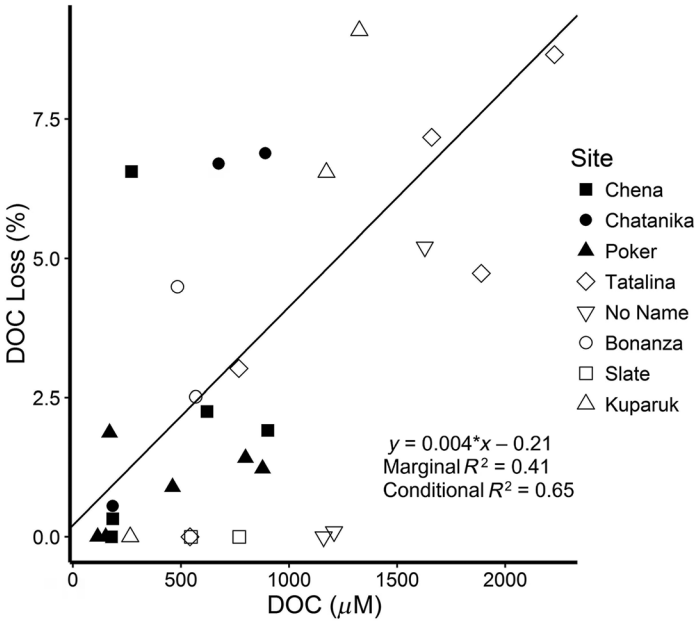


**Fig. 5.** Correlation of ambient DOC concentration and total percent loss of DOC during incubations of streamwater. Site was included as a random effect.

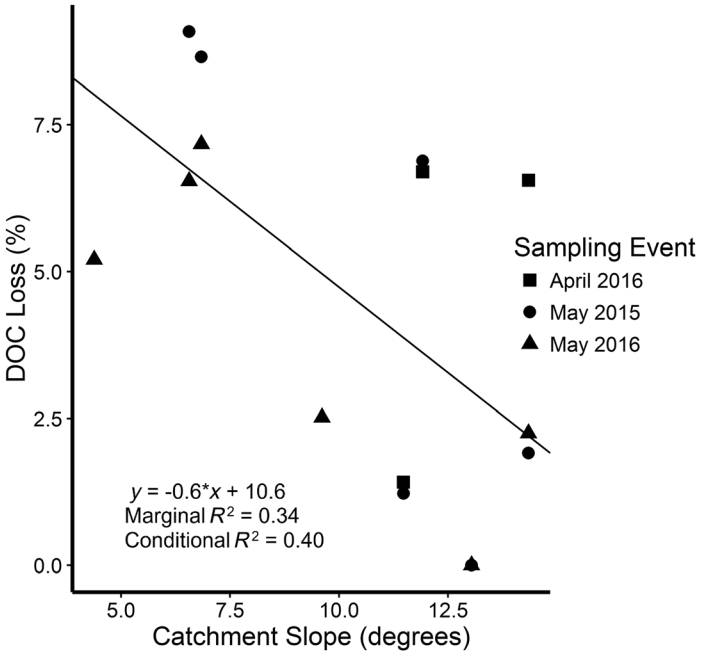


**Fig. 6.** Correlation of mean catchment slope and total percent loss of DOC in unfertilized assays during April and May. Each point represents a single stream. Sampling date was included as a random effect.

controls (Supporting Information Table 3). Examination of the interaction of sampling event and nutrient treatment indicated that P increased decomposition most during April and May, with significant increases in DOC loss from the P and N + P treatments compared to control, as determined by Bonferroni-corrected multiple comparisons of fertilized assays to unfertilized controls (Fig. 4). There was no significant effect of N fertilization on biolability at any time when comparing fertilized assays to controls within each site.

Enhancement of biolability due to nutrient fertilization was more likely when DOC concentration was greatest. Logistic regression models indicated that DOC concentration was the strongest predictor of N response and additional models of comparable explanatory power indicated a negative effect of ambient streamwater C : P, C : N, and the protein-like Component 4 on N response. Component 1 (humic-like), and DON concentration had positive effects on N response (Supporting Information Table 4). Logistic models describing the P response of biolability explained little variance ($R^2 < 0.1$).

## Discussion

Large loads of DOC transported by high-latitude rivers may contribute to a positive feedback with climate warming if the organic matter is readily decomposed (Vonk et al. 2013), or may contribute to stability in the C cycle, by promoting export of recalcitrant compounds to coastal waters. We examined the chemical and catchment-level factors influencing decomposition of DOM in high-latitude rivers, and quantified regional and intra-annual variation in stream chemistry to improve understanding of the mechanisms that drive biolability. Recalcitrant, humic-like functional groups dominated the DOM pool (Figs. 2–4), indicating that DOM leached from the large store of terrestrial organic matter contributes to the observed intra-annual stability and regional homogeneity in export of DOM. Biolability of DOC was generally low, and both concentration and relative biolability of DOC increased during snowmelt when P addition stimulated decomposition (Fig. 4), supporting the hypothesis that nutrient limitation constrains decomposition in high-latitude rivers. Thus, efficient export of DOM from rivers to coasts constrains the riverine flux of C to the atmosphere, but increased availability of P (Toohey et al. 2016) or labile sources of C (Vonk et al. 2013) are expected to enhance decomposition and release $CO_2$ from rivers.

### Sources of DOM to rivers

Temporal patterns in DOM composition corresponded to seasonal trends in the hydrology of high-latitude catchments (Fig. 2). Greater SUVA values and lower SR, BIX, and FI values observed during snowmelt (April–May) compared to other times (Fig. 2g,j,k) represent flushing of DOM that is aromatic, of high-molecular weight, and terrestrially derived. Shallow soil horizons in high-latitude regions are rich in organic C (Hugelius et al. 2014), and DOM in pore water from these soils is highly aromatic and dominated by

compounds of high molecular weight (Wickland et al. 2007; Frey et al. 2016). Leaf litter is a likely contributor to DOM flushed during snowmelt (Spencer et al. 2008), as evidenced in the present study by a high relative contribution of EEMs Component 5 during May of both years of the study (Fig. 3), which was prevalent in leachates from boreal plant species (mean fluorescence loading = 41%; Mutschlecner et al. 2017).

Although DOM was most aromatic, humic, and dominated by terrestrial sources during snowmelt, DOM in rivers was sourced largely from soil organic matter throughout the year. Indicators of DOM sourced from decomposed soil organic matter persisted throughout the study period, including high SUVA values, HIX values near 1, and dominance of EEMs Components 1 and 2 (Fig. 2h,j). Stronger declines in terrestrially derived DOM following snowmelt in other high-latitude rivers (Spencer et al. 2008; Mann et al. 2012) as well as in the largest rivers of Interior Alaska (Wickland et al. 2012) contrast with the muted seasonality observed in the present dataset. Seasonal decline in concentration of humic DOM from snowmelt through winter is hypothesized to result from increased relative input of groundwater and flows through relatively organic-poor mineral soils to rivers (O'Donnell et al. 2012). Persistence of humic DOM in rivers might occur if frozen ground does not permit flowpaths to deepen into mineral soils, or if the organic layer is particularly thick due to Yedoma deposits or ecosystems that promote development of the organic layer (Chapin et al. 2010; Strauss et al. 2017). Mineral ions, a proxy for inputs of deep flows (O'Donnell et al. 2010), increased in concentration from snowmelt through winter in some of the rivers studied here (Supporting Information Fig. 5), but on average temporal patterns in this proxy were not significant (Fig. 2b). Thus, DOM was largely delivered to rivers via shallow flowpaths throughout the year or the study catchments encompass deep organic layers that provide a constant source of humic DOM to rivers.

**Low biolability across sites and seasons**

The majority of riverine DOM observed across the arctic-boreal gradient and over an annual period was recalcitrant to biological decomposition. Although the range in biolability for this study (0–42%) agrees with other estimates for arctic and boreal rivers (0–53%; Vonk et al. 2015), mean biolability measured in the present study was 4%, in the lower range of previously reported values. Explanations for the low average biolability observed in the present study include: (1) the timing of sample collection and (2) variation contributed by catchment size or physical features.

Most previous studies have focused on the snowmelt and growing seasons, whereas our study included winter, an under sampled period characterized by low biolability. In addition to declines in the humic content of DOM during winter as previously described, DOC concentration was lowest during winter. Given that DOC concentration was the primary correlate of biolability (Fig. 5), low DOC concentration in winter likely contributes to its recalcitrance.

Consensus is emerging that biolability decreases with increasing contributing area, because increasing water residence time results in longer exposure to biological and photochemical processes that remove labile fractions (Vonk et al. 2015; Catalán et al. 2016; Casas-Ruiz et al. 2017). Our study of $5^{th}$–$7^{th}$ order rivers precludes a test of this hypothesis, but greater lability in headwater tributaries reported by previous studies than observed in the present dataset of larger rivers might support this hypothesis. Balcarczyk et al. (2009) estimated that in a headwater tributary of one of the rivers reported here (Poker Creek), 6–17% of DOC was labile, whereas we estimated that < 1% was biolabile in the mainstem in the same season. White et al. (2008) found maximum absolute loss of DOC of nearly 7 mg C/L for headwater streams within the same watershed, whereas maximum absolute loss for this study was 2.4 mg C/L. In contrast to this apparent support for the hypothesis relating lability to river size, some estimates of biolability were greater for the Yukon River and its major tributaries (Wickland et al. 2012) than we report for smaller rivers in the Yukon basin. Spatial heterogeneity among catchments could impart further variation in biolability that obscures the expected pattern with river size. For example, presence of glaciers may explain the elevated biolability previously observed for the Yukon and its major tributaries, as glaciated watersheds export DOM of high biolability relative to nonglaciated watersheds (Hood et al. 2009), whereas the rivers sampled in the present study do not include glaciers. Additionally, we observed greatest biolability in catchments of lowest slope (Fig. 6) which might occur because low topographic relief enhances opportunity for leaching of organic matter, yielding higher concentrations of DOC characterized by greater humic content (Harms et al. 2016).

Low biolability even when nutrient limitation was relieved by fertilization (mean biolability for fertilized treatments = 5%, Fig. 4) suggests that decomposition in the study region is limited more strongly by molecular composition of DOM than by nutrients. Labile C limits microbial respiration in boreal rivers, particularly in winter when terrestrial inputs are low (Burrows et al. 2017). Correlational evidence supports links between the composition of DOM and biolability although contrasting patterns emerge depending upon the analytical techniques applied to measure DOM composition and the breadth of DOM sources considered. For example, low molecular weight compounds fuel bacterial growth in boreal rivers and are rapidly respired following thaw and leaching of organic-rich permafrost (Berggren et al. 2010; Drake et al. 2015). In contrast, higher average molecular weight of the DOM pool yielded greater biolability in rivers of Siberia (Frey et al. 2016), and high relative abundance of humic and aromatic functional groups

correlated with biolability in the same region (Mann et al. 2012) as well as in the boreal forest (Kellerman et al. 2015). Despite the annual time scale and regional spatial extent of the present study, low variation in biolability and composition of DOM precluded detection of correlations between molecular composition and biolability. However, highest rates of decomposition were observed during snowmelt (Fig. 4), when composition of the DOM pool differed significantly from other sampled dates and reflected highest concentrations of aromatic, humic molecules derived from soil organic matter (Figs. 2, 3).

**Phosphorus limitation of biolability**

Fertilization assays indicated that nutrient limitation of decomposition occurred only during the snowmelt period, and that P limited decomposition of DOM (Fig. 4). In addition, increased biolability in response to N addition relative to unamended controls was more likely when ambient P was more available (i.e., when C : P ratios were lower; Supporting Information Table 4), demonstrating potential secondary limitation by N. Observation of P limitation in laboratory assays concurs with increasing evidence from laboratory and field-based studies indicating P limitation of C cycling processes in high-latitude rivers. C : N and C : P ratios observed in this and previous studies of high-latitude rivers indicate the potential for P limitation or co-limitation by N and P (Fellman et al. 2008; Holmes et al. 2012). Further, co-occurrence of concentrations of bioavailable DOC and TDP that both exceeded the study-wide means by several-fold in a sample of overflow from the Kuparuk River during winter provide supporting evidence regarding the role of P. Respiration was positively correlated with ambient P concentration in bioassays of a river in the Siberian arctic (Mann et al. 2014) and addition of P enhanced decomposition of boreal DOM in laboratory experiments (Kragh et al. 2008). Fertilization of the Kuparuk River with P stimulated heterotrophic activity directly and due to release of labile C from enhanced primary production (Peterson et al. 1993). Thus, P availability likely constrains the release of $CO_2$ from high-latitude rivers. However, low biolability even with the addition of P indicates that riverine DOM is largely recalcitrant due to its molecular composition.

## Conclusions

The DOM pool of high-latitude rivers spanning a regional spatial extent and annual sampling period was relatively stable in molecular composition and recalcitrant to microbial decomposition. Soil organic matter that has accumulated over millennia in high-latitude ecosystems contributes stability to the C cycle of aquatic ecosystems by providing a large source of humic DOM. Soil organic matter buffers DOM export against shorter-term changes in sources such as rate of primary production or dominant plant species (Schuur et al. 2008; Chapin et al. 2010). However, degrading permafrost could increase flux of $CO_2$ from high-latitude rivers due to altered molecular structure and enhanced biolability of permafrost-derived DOM relative to shallow organic soils (Abbott et al. 2014; Spencer et al. 2015; Selvam et al. 2017). Observed coupling of the C cycle with nutrient cycles via P limitation of decomposition suggests that reduced stability in the C cycle might result if nutrient availability increases and reduces constraints on decomposition. Shifting the fate of riverine DOM from export to respiration can have a substantial effect on regional and global C budgets (Kling et al. 1991; Butman et al. 2016). Monitoring long-term changes in nutrient concentrations and molecular composition of DOM in high-latitude rivers, and representing coupling of C and P cycles in C-cycle models might best anticipate loss of stability in the riverine contribution to the high-latitude C cycle.

## References

Abbott, B., J. R. Larouche, J. B. Jones, W. B. Bowden, and A. W. Balser. 2014. Elevated dissolved organic carbon biodegradability from thawing and collapsing permafrost. J. Geophys. Res. Biogeosci. **119**: 2049–2063. doi:10.1002/2014JG002678

Balcarczyk, K. L., J. B. Jones, R. Jaffé, and N. Maie. 2009. Stream dissolved organic matter bioavailability and composition in watersheds underlain with discontinuous permafrost. Biogeochemistry **94**: 255–270. doi:10.1007/s10533-009-9324-x

Barton, K. 2016. MuMIn: Multi-model inference. R package version 1.15.6; [accessed 2018 February 8]. Available from https://CRAN.R-project.org/package=MuMIn

Bates, D., M. Mächler, B. Bolker, and S. C. Walker. 2015. Fitting linear mixed-effects models using lme4. J. Stat. Softw. **67**: 1–51. doi:10.18637/jss.v067.i01

Berggren, M., H. Laudon, M. Haei, L. Ström, and M. Jansson. 2010. Efficient aquatic bacterial metabolism of dissolved low-molecular-weight compounds from terrestrial sources. ISME J. **4**: 408–416. doi:10.1038/ismej.2009.120

Bonanza Creek LTER Climate Database. 2016. Bonanza Creek LTER - University of Alaska Fairbanks (http://www.lter.uaf.edu). National Science Foundation Long-Term Ecological Research program Grant number DEB-1026415 and USDA Forest Service, Pacific Northwest Research Station Agreement # RJVA-PNW-01-J.

Brabets, T. B., B. Wang, and R. M. Meade. 2000. Environmental and hydrologic overview of the Yukon River Basin, Alaska and Canada. Water-Resources Investigations Report 99–4204. U.S. Geological Survey.

Brabets, T. P., and M. A. Walvoord. 2009. Trends in streamflow in the Yukon River Basin from 1944 to 2005 and the influence of the Pacific Decadal Oscillation. J. Hydrol. **371**: 108–119. doi:10.1016/j.jhydrol.2009.03.018

Burrows, R. M., H. Laudon, B. G. McKie, and R. A. Sponseller. 2017. Seasonal resource limitation of heterotrophic biofilms

in boreal streams. Limnol. Oceanogr. **62**: 164–176. doi:10.1002/lno.10383

Butman, D., S. Stackpoole, E. Stets, C. P. McDonald, D. W. Clow, and R. G. Striegl. 2016. Aquatic carbon cycling in the conterminous United States and implications for terrestrial carbon accounting. Proc. Natl. Acad. Sci. USA **113**: 58–63. doi:10.1073/pnas.1512651112

Casas-Ruiz, J. P., and others. 2017. A tale of pipes and reactors: Controls on the in-stream dynamics of dissolved organic matter in rivers. Limnol. Oceanogr. **62**: S85–S94. doi:10.1002/lno.10471

Catalán, N., R. Marcé, D. N. Kothawala, and L. J. Tranvik. 2016. Organic carbon decomposition rates controlled by water retention time across inland waters. Nat. Geosci. **9**: 501–507. doi:10.1038/ngeo2720

Chapin, F. S., and others. 2010. Resilience of Alaska's boreal forest to climate change. Can. J. For. Res. **40**: 1360–1370. doi:10.1139/X10-074

Cory, R. M., and D. M. McKnight. 2005. Fluorescence spectroscopy reveals ubiquitous presence of oxidized and reduced quinones in dissolved organic matter. Environ. Sci. Technol. **39**: 8142–8149. doi:10.1021/es0506962

Cory, R. M., J. M. Purcell, and A. G. Marshall. 2010. Singlet oxygen in the coupled photochemical and biochemical oxidation of dissolved organic matter. Environ. Sci. Technol. **44**: 3683–3689. doi:10.1021/es902989y

Cory, R. M., and L. A. Kaplan. 2012. Biological lability of streamwater fluorescent dissolved organic matter. Limnol. Oceanogr. **57**: 1347–1360. doi:10.4319/lo.2012.57.5.1347

Dainard, P. G., C. Guéguen, N. McDonald, and W. J. Williams. 2015. Photobleaching of fluorescent dissolved organic matter in Beaufort Sea and North Atlantic Subtropical Gyre. Mar. Chem. **177**: 630–637. doi:10.1016/j.marchem.2015.10.004

Drake, T. W., K. P. Wickland, R. G. M. Spencer, D. M. McKnight, and R. G. Striegl. 2015. Ancient low–molecular-weight organic acids in permafrost fuel rapid carbon dioxide production upon thaw. Proc. Natl. Acad. Sci. USA **112**: 13946–13951. doi:10.1073/pnas.1511705112

Euskirchen, E. S., A. D. McGuire, F. S. Chapin, III, and T. S. Rupp. 2010. The changing effects of Alaska's boreal forests on the climate system. Can. J. For. Res. **40**: 1336–1324. doi:10.1139/X09-209

Fellman, J. B., D. V. D'Amore, E. Hood, and R. D. Boone. 2008. Fluorescence characteristics and biodegradability of dissolved organic matter in forest and wetland soils from coastal temperate watersheds in southeast Alaska. Biogeochemistry **88**: 169–184. doi:10.1007/s10533-008-9203-x

Fellman, J. B., E. Hood, D. V. D'Amore, R. T. Edwards, and D. White. 2009a. Seasonal changes in the chemical quality and biodegradability of dissolved organic matter exported from soils to streams in coastal temperate rainforest watersheds. Biogeochemistry **95**: 277–293. doi:10.1007/s10533-009-9336-6

Fellman, J. B., E. Hood, R. T. Edwards, and J. B. Jones. 2009b. Uptake of allochthonous dissolved organic matter from soil and salmon in coastal temperate rainforest streams. Ecosystems **12**: 747–759. doi:10.1007/s10021-009-9254-4

Ferrians, O. 1998. Permafrost map of Alaska, USA, Version 1. National Snow and Ice Data Center (NSIDC).

Finlay, J., J. Neff, S. Zimov, A. Davydova, and S. Davydov. 2006. Snowmelt dominance of dissolved organic carbon in high-latitude watersheds: Implications for characterization and flux of river DOC. Geophys. Res. Lett. **33**: L10401. doi:10.1029/2006GL025754

Fouché, J., M. J. Lafrenière, K. Rutherford, and S. Lamoureux. 2017. Seasonal hydrology and permafrost disturbance impacts on dissolved organic matter composition in High Arctic headwater catchments. Arct. Sci. **3**: 378–405. doi:10.1139/as-2016-0031

Frey, K. E., W. V. Sobczak, P. J. Mann, and R. M. Holmes. 2016. Optical properties and bioavailability of dissolved organic matter along a flow-path continuum from soil pore waters to the Kolyma River mainstem, East Siberia. Biogeosciences **13**: 2279–2290. doi:10.5194/bg-13-2279-2016

Godwin, C. M., E. A. Whitaker, and J. B. Cotner. 2017. Growth rate and resource imbalance interactively control biomass stoichiometry and elemental quotas of aquatic bacteria. Ecology **98**: 820–829. doi:10.1002/ecy.1705

Harms, T. K., J. W. Edmonds, H. Genet, I. F. Creed, D. Aldred, A. Balser, and J. B. Jones. 2016. Catchment influence on nitrate and dissolved organic matter in Alaskan streams across a latitudinal gradient. J. Geophys. Res. Biogeosci. **121**: 350–369. doi:10.1002/2015JG003201

Helms, J. R., A. Stubbins, J. D. Ritchie, E. C. Minor, D. J. Kieber, and K. Mopper. 2008. Absorption spectral slopes and slope ratios as indicators of molecular weight, source, and photobleaching of chromophoric dissolved organic matter. Limonol. Oceanogr. **53**: 955–969. doi:10.4319/lo.2008.53.3.0955

Hessen, D. O., and T. R. Anderson. 2008. Excess carbon in aquatic organisms and ecosystems: Physiological, ecological, and evolutionary implications. Limnol. Oceanogr. **53**: 1685–1696. doi:10.4319/lo.2008.53.4.1685

Holmes, R. M., J. W. McClelland, P. A. Raymond, B. B. Frazer, B. J. Peterson, and M. Stieglitz. 2008. Lability of DOC transported by Alaskan rivers to the Arctic Ocean. Geophys. Res. Lett. **35**: L03402. doi:10.1029/2007GL032837

Holmes, R. M., and others. 2012. Seasonal and annual fluxes of nutrients and organic matter from large rivers to the arctic ocean and surrounding seas. Estuaries Coast. **35**: 369–382. doi:10.1007/s12237-011-9386-6

Hood, E., J. Fellman, R. G. M. Spencer, P. J. Hernes, R. Edwards, D. D'Amore, and D. Scott. 2009. Glaciers as a source of ancient and labile organic matter to the marine environment. Nature **462**: 1044–1047. doi:10.1038/nature08580

Hugelius, G., and others. 2014. Estimated stocks of circumpolar permafrost carbon with quantified uncertainty

ranges and identified data gaps. Biogeosciences **11**: 6573–6593. doi:10.5194/bg-11-6573-2014

Huguet, A., L. Vacher, S. Relexans, S. Saubusse, J. M. Froidefond, and E. Parlanti. 2009. Properties of fluorescent dissolved organic matter in the Gironde Estuary. Org. Geochem. **40**: 706–719. doi:10.1016/j.orggeochem.2009.03.002

Jones, J. B., K. C. Petrone, J. C. Finlay, L. D. Hinzman, and W. R. Bolton. 2005. Nitrogen loss from watersheds of interior Alaska underlain with discontinuous permafrost. Geophys. Res. Lett. **32**: L02401. doi:10.1029/2004GL021734

Kellerman, A. M., D. N. Kothawala, T. Dittmar, and L. J. Tranvik. 2015. Persistence of dissolved organic matter in lakes related to its molecular characteristics. Nat. Geosci. **8**: 454–459. doi:10.1038/NGEO2440

Kiikkilä, O., A. Smolander, and V. Kitunen. 2013. Degradability, molecular weight and adsorption properties of dissolved organic carbon and nitrogen leached from different types of decomposing litter. Plant Soil **373**: 787–798. doi:10.1007/s11104-013-1837-3

Kling, G. W., G. W. Kipphut, and M. C. Miller. 1991. Arctic lakes and streams as gas conduits to the atmosphere: Implications for tundra carbon budgets. Science **251**: 298–301. doi:10.1126/science.251.4991.298

Köchy, M., R. Hiederer, and A. Freibauer. 2015. Global distribution of soil organic carbon – part 1: Masses and frequency distributions of SOC stocks for the tropics, permafrost regions, wetlands, and the world. Soil **1**: 351–365. doi:10.5194/soil-1-351-2015

Kothawala, D. N., C. A. Stedmon, R. A. Muller, G. A. Weyhenmeyer, S. J. Kohler, and L. J. Tranvik. 2014. Controls of dissolved organic matter quality: Evidence from a large-scale boreal lake survey. Glob. Chang. Biol. **20**: 1101–1114. doi:10.1111/gcb.12488

Kragh, T., M. Søndergaard, and L. Tranvik. 2008. Effect of exposure to sunlight and phosphorus-limitation on bacterial degradation of coloured dissolved organic matter (CDOM) in freshwater. FEMS Microbiol. Ecol. **64**: 230–239. doi:10.1111/j.1574-6941.2008.00449.x

Larouche, J. R., B. W. Abbott, W. B. Bowden, and J. B. Jones. 2015. The role of watershed characteristics, permafrost thaw, and wildfire on dissolved organic carbon biodegradability and water chemistry in Arctic headwater streams. Biogeosciences **12**: 4021–4233. doi:10.5194/bgd-12-4021-2015

Mann, P. J., A. Davydova, N. Zimov, R. G. M. Spencer, S. Davydov, E. Bulygina, S. Zimov, and R. M. Holmes. 2012. Controls on the composition and lability of dissolved organic matter in Siberia's Kolyma River basin. J. Geophys. Res. Biogeosci. **117**: 1–15. doi:10.1029/2011JG001798

Mann, P. J., and others. 2014. Evidence for key enzymatic controls on metabolism of Arctic river organic matter. Glob. Chang. Biol. **20**: 1089–1100. doi:10.1111/gcb.12416

Mann, P. J., T. I. Eglinton, C. P. McIntyre, N. Zimov, A. Davydova, J. E. Vonk, R. M. Holmes, and R. G. M. Spencer. 2015. Utilization of ancient permafrost carbon in headwaters of Arctic fluvial networks. Nat. Commun. **6**: 1–7. doi:10.1038/ncomms8856

McClelland, J. W., M. Stieglitz, F. Pan, R. M. Holmes, and B. J. Peterson. 2007. Recent changes in nitrate and dissolved organic carbon export from the upper Kuparuk River, North Slope, Alaska. J. Geophys. Res. **112**: G04S60. doi:10.1029/2006JG000371

McKnight, D. M., E. W. Boyer, P. K. Westerhoff, P. T. Doran, T. Kulbe, and D. T. Andersen. 2001. Spectrofluorometric characterization of dissolved organic matter for indication of precursor organic material and aromaticity. Limnol. Oceanogr. **46**: 38–48. doi:10.4319/lo.2001.46.1.0038

Murphy, J., and J. P. Riley. 1962. A modified single solution method for the determination of phosphate in natural waters. Anal. Chim. Acta **27**: 31–36. doi:10.1016/S0003-2670(00)88444-5

Murphy, K. R., C. A. Stedmon, P. Wenig, and R. Bro. 2014. OpenFluor- an online spectral library of auto-fluorescence by organic compounds in the environment. Anal. Methods **6**: 658–661. doi:10.1039/C3AY41935E

Mutschlecner, A. E., J. J. Guerard, J. B. Jones, and T. K. Harms. 2017. Phosphorus enhances uptake of dissolved organic matter in boreal streams. Ecosystems. In press. doi:10.1007/s10021-017-0177-1

O'Donnell, J. A., G. R. Aiken, E. S. Kane, and J. B. Jones. 2010. Source water controls on the character and origin of dissolved organic matter in streams of the Yukon River basin, Alaska. J. Geophys. Res. Biogeosci. **115**: 1–12. doi:10.1029/2009JG001153

O'Donnell, J. A., G. R. Aiken, M. A. Walvoord, and K. D. Butler. 2012. Dissolved organic matter composition of winter flow in the Yukon River basin: Implications of permafrost thaw and increased groundwater discharge. Global Biogeochem. Cycles. **26**: 1–18. doi:10.1029/2012GB004341

O'Donnell, J. A., G. R. Aiken, D. K. Swanson, S. Panda, K. D. Butler, and A. P. Baltensperger. 2016. Dissolved organic matter composition of Arctic rivers: Linking permafrost and parent material to riverine carbon. Global Biogeochem. Cycles **30**: 1811–1826. doi:10.1002/2016GB005482

Ohno, T. 2002. Fluorescence inner-filtering correction for determining the humification index of dissolved organic matter. Environ. Sci. Technol. **36**: 742–746. doi:10.1021/es0155276

Parlanti, E., K. Wörz, L. Geoffroy, and M. Lamotte. 2000. Dissolved organic matter fluorescence spectroscopy as a tool to estimate biological activity in a coastal zone submitted to anthropogenic inputs. Org. Geochem. **31**: 1765–1781. doi:10.1016/S0146-6380(00)00124-8

Peterson, B. J., and others. 1993. Biological responses of a tundra river to fertilization. Ecology **74**: 653–672. doi:10.2307/1940794

Qualls, R. G., and B. L. Haines. 1992. Biodegradability of dissolved organic matter in forest throughfall, soil solution,

and stream water. Soil Sci. Soc. Am. J. **56**: 578–586. doi:10.2136/sssaj1992.03615995005600020038x

R Core Team. 2016. R: A language and environment for statistical computing. R Foundation for Statistical Computing; [accessed 2018 February 8]. Available from www.r-project.org

Raymond, P. A., and others. 2007. Flux and age of dissolved organic carbon exported to the Arctic Ocean: A carbon isotopic study of the five largest arctic rivers. Global Biogeochem. Cycles **21**: GB4011. doi:10.1029/2007GB002934

Schuur, E., and others. 2008. Vulnerability of permafrost carbon to climate change: Implications for the global carbon cycle. Bioscience **58**: 701–714. doi:10.1641/B580807

Selvam, B. P., and others. 2017. Degradation potentials of dissolved organic carbon (DOC) from thawed permafrost peat. Sci. Rep. **7**: 45811–45819. doi:10.1038/srep45811

Shutova, Y., A. Baker, J. Bridgeman, and R. K. Henderson. 2014. Spectroscopic characterisation of dissolved organic matter changes in drinking water treatment: From PARAFAC analysis to online monitoring wavelengths. Water Res. **54**: 159–169. doi:10.1016/j.watres.2014.01.053

Sinsabaugh, R. L., S. Manzoni, D. L. Moorhead, and A. Richter. 2013. Carbon use efficiency of microbial communities: Stoichiometry, methodology and modelling. Ecol. Lett. **16**: 930–939. doi:10.1111/ele.12113

Solórzano, L. 1969. Determination of ammonia in natural waters by the phenolhypochlorite method. Limnol. Oceanogr. **14**: 799–801. doi:10.4319/lo.1969.14.5.0799

Spencer, R. G. M., G. R. Aiken, K. P. Wickland, R. G. Striegl, and P. J. Hernes. 2008. Seasonal and spatial variability in dissolved organic matter quantity and composition from the Yukon River basin, Alaska. Global Biogeochem. Cycles. **22**: GB4002. doi:10.1029/2008GB003231

Spencer, R. G. M., P. J. Mann, T. Dittmar, T. I. Eglinton, C. McIntyre, R. M. Holmes, N. Zimov, and A. Stubbins. 2015. Detecting the signature of permafrost thaw in Arctic rivers. Geophys. Res. Lett. **42**: 2830–2835. doi:10.1002/2015GL063498

Stackpoole, S. M., D. E. Butman, D. W. Clow, K. L. Verdin, B. V. Gaglioti, H. Genet, and R. G. Striegl. 2017. Inland waters and their role in the carbon cycle of Alaska. Ecol. Appl. **27**: 1403–1420. doi:10.1002/eap.1552

Stedmon, C. A., S. Markager, and R. Bro. 2003. Tracing dissolved organic matter in aquatic environments using a new approach to fluorescence spectroscopy. Mar. Chem. **82**: 239–254. doi:10.1016/S0304-4203(03)00072-0

Stedmon, C. A., and R. Bro. 2008. Characterizing dissolved organic matter fluorescence with parallel factor analysis: A tutorial. Limnol. Oceanogr.: Methods **6**: 572–579. doi:10.4319/lom.2008.6.572

Stone, R. S., E. G. Dutton, J. M. Harris, and D. Longenecker. 2002. Earlier spring snowmelt in northern Alaska as an indicator of climate change. J. Geophys. Res. **107**: ACL 10-1–ACL 10–13. doi:10.1029/2000JD000286

Strauss, J., and others. 2017. Deep Yedoma permafrost: A synthesis of depositional characteristics and carbon vulnerability. Earth Sci. Rev. **172**: 75–86. doi:10.1016/j.earscirev.2017.07.007

Striegl, R. G., G. R. Aiken, M. M. Dornblaser, P. A. Raymond, and K. P. Wickland. 2005. A decrease in discharge-normalized DOC export by the Yukon River during summer through autumn. Geophys. Res. Lett. **32**: L21413. doi:10.1029/2005GL024413

Striegl, R. G., M. M. Dornblaser, G. R. Aiken, K. P. Wickland, and P. A. Raymond. 2007. Carbon export and cycling by the Yukon, Tanana, and Porcupine rivers, Alaska, 2001–2005. Water Resour. Res. **43**: W02411. doi:10.1029/2006WR005201

Toohey, R. C., N. M. Herman-Mercer, P. F. Schuster, E. Mutter, and J. C. Koch. 2016. Multi-decadal increases in the Yukon River Basin of chemical fluxes as indicators of changing flowpaths, groundwater, and permafrost. Geophys. Res. Lett. **43**: 12120–12130. doi:10.1002/2016GL070817

Toolik Environmental Data Center Team. 2016. Meteorological monitoring program at Toolik, Alaska. Toolik Field Station, Institute of Arctic Biology, Univ. of Alaska Fairbanks. Available from http//toolik.alaska.edu/edc/abiotic_monitoring/data_query.php

Vonk, J. E., and others. 2013. High biolability of ancient permafrost carbon upon thaw. Geophys. Res. Lett. **40**: 2689–2693. doi:10.1002/grl.50348

Vonk, J. E., S. E. Tank, P. J. Mann, R. G. M. Spencer, C. C. Treat, R. G. Striegl, B. W. Abbott, and K. P. Wickland. 2015. Biodegradability of dissolved organic carbon in permafrost soils and aquatic systems: A meta-analysis. Biogeosciences **12**: 6915–6930. doi:10.5194/bg-12-6915-2015

Weishaar, J., G. Aiken, B. Bergamaschi, M. Fram, R. Fujii, and K. Mopper. 2003. Evaluation of specific ultra-violet absorbance as an indicator of the chemical content of dissolved organic carbon. Environ. Sci. Technol. **37**: 4702–4708. doi:10.1021/es030360x

White, D., V. Autier, K. Yoshikawa, J. Jones, and S. Seelen. 2008. Using DOC to better understand local hydrology in a subarctic watershed. Cold Reg. Sci. Technol. **51**: 68–75. doi:10.1016/j.coldregions.2007.08.005

Wickland, K. P., J. C. Neff, and G. R. Aiken. 2007. Dissolved organic carbon in Alaskan boreal forest: Sources, chemical characteristics, and biodegradability. Ecosystems **10**: 1323–1340. doi:10.1007/s10021-007-9101-4

Wickland, K. P., G. R. Aiken, K. Butler, M. M. Dornblaser, R. G. M. Spencer, and R. G. Striegl. 2012. Biodegradability of dissolved organic carbon in the Yukon River and its tributaries: Seasonality and importance of inorganic nitrogen. Global Biogeochem. Cycles. **26**: GB0E03. doi:10.1029/2012GB004342

Wilson, H. F., and M. A. Xenopoulos. 2009. Effects of agricultural land use on the composition of fluvial dissolved

organic matter. Nat. Geosci. **2**: 37–41. doi:10.1038/ngeo391

## Acknowledgments

We thank personnel from the Bonanza Creek Long-Term Ecological Research program and Toolik Field Station for assistance with data collection, particularly B. Van Dam, K. Olson, and A. Cocallas. Two reviewers provided comments that improved the manuscript. Funding was provided by the Institute of Arctic Biology, Department of Biology & Wildlife (including Nicholas F. Hughes Memorial Scholarship to AEM), and the Bonanza Creek Long-Term Ecological Research program (funded jointly by NSF grant DEB-1026415 and USDA Forest Service, Pacific Northwest Research Station grant PNW01-JV-11261952-231).

## Conflict of Interest

None declared.

*Submitted 11 April 2017*
*Revised 11 September 2017; 15 January 2018*
*Accepted 01 February 2018*

*Associate editor: Kimberly Wickland*